Supporting Information

The Impact of Fiber Arrangement and Advective Transport in Porous Ag-TRAB Electrodes

Authors: Nicholas R. Cross[a], Matthew J. Rau[b,1], Derek M. Hall[c,d], Serguei N. Lvov[c,d,e], and Bruce E. Logan[a,f]

[a]Department of Chemical Engineering, Pennsylvania State University, University Park, PA 16802, USA
[b]Department of Mechanical Engineering, Pennsylvania State University, University Park, PA 16802, USA
[c]The EMS Energy Institute, Pennsylvania State University, University Park, PA 16802, USA
[d]Department of Energy and Mineral Engineering, Pennsylvania State University, University Park, PA 16802, USA
[e]Department of Materials Science and Engineering, Pennsylvania State University, University Park, PA 16802, USA
[f]Department of Civil and Environmental Engineering, Pennsylvania State University, University Park, PA 16802, USA

[1] Corresponding author: matthew.rau@psu.edu

Section 1: Estimation of Parameters Using a Rotating Disk Electrode

In order to estimate the exchange current density and transfer coefficient to be used for the simulations, Koutecky-Levich analysis was performed on the rotating disk electrode experiment results. For this analysis, the ammonium nitrate concentration was 5 M, the silver nitrate concentration were 1, 5, 10, 50, and 100 mmol, and the rotation rates were 500 and 1000 rpm. A potential range of 40-60 mV below the equilibrium potential was used for this analysis. In literature, values for the minimum of the potential range for this vary from 10 to 118 mV based off the value for which the Tafel approximation to be valid [1–3]. For the range used, it was estimated that the reverse (anodic) reaction contributed between 10-25% of the current output.

The current density at infinite rotation rate was estimated using

$$\frac{1}{j_\omega(\eta)} = \frac{1}{j_\infty(\eta)} + \left(\frac{1}{j_\infty(\eta)}\right)\frac{B}{\omega^{\frac{1}{2}}}, \tag{S1}$$

where, j_ω is the current at a specified rotation rate, j_∞ is the estimated current at infinite rotation rate, B is the Levich constant, and ω is the rotation rate. This current was then plotted against the overpotential, and the data fitted to extrapolate the transfer coefficient, α_c, and the exchange current density, j_0, using

$$log_{10} j_\infty = -\eta \frac{\alpha_c F}{RT\ln(10)} + log_{10} j_0. \tag{S2}$$

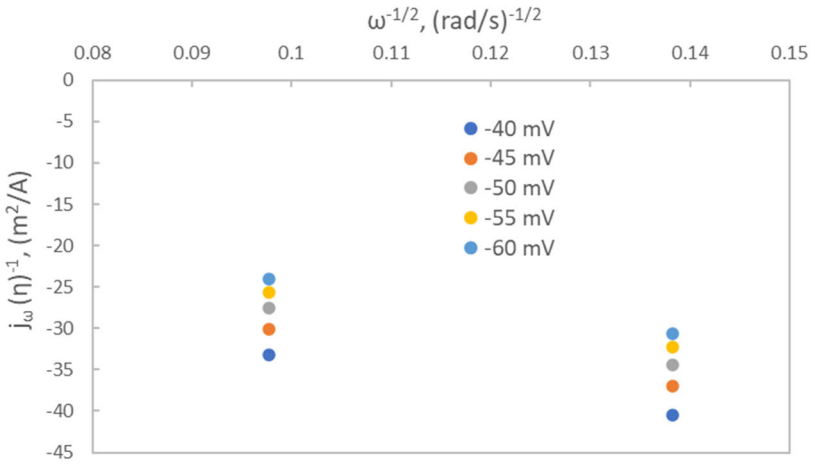

a)

b)

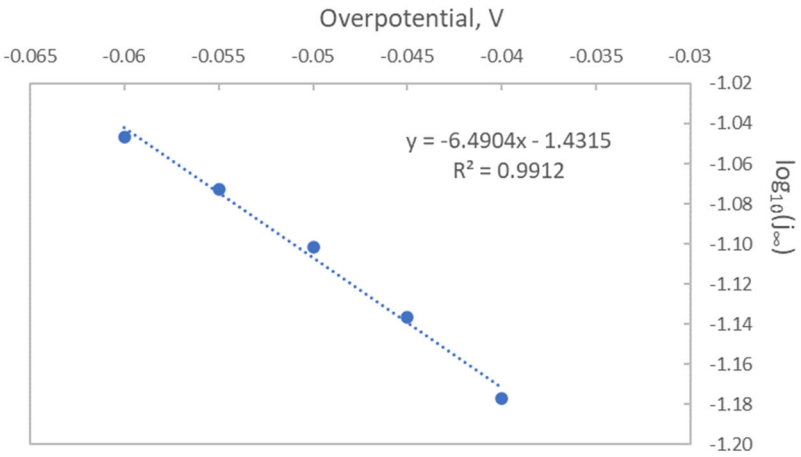

Figure S.1: Sample Koutecky plots created for the data obtained for the 100 mmol concentration experiments.

Rate constants were calculated from the extrapolated exchange current densities using

$$j_0 = nFk_0\left(c_a^{1-\alpha_c}\, c_o^{\alpha_c}\right), \tag{S3}$$

where k_0 is the rate constant. For this equation, c_o was assumed to be 1 since the species was silver metal.

Table S.1: Summary of fitted parameters from the Koutecky-Levich analysis

Parameter	**1 mmol**	**5 mmol**	**10 mmol**	**50 mmol**	**100 mmol**
alpha	0.17	0.16	0.21	0.31	0.38
j0 (A/cm^2)	0.0005	0.0020	0.0037	0.0174	0.0370
k0 (cm/s)	0.0005	0.0006	0.0003	0.00016	0.00011

Table S.1 shows all the kinetic parameters that resulted from the Koutecky-Levich analysis. The exchange current densities and rate constants were lower than that of previous literature results; however, the previous literature results used different concentrations for different chemistries, so a direct comparison is not valid for these values. The transfer coefficients for 1, 5, and 10 mmol were lower than that of previous literature values, and their being well below 0.5 indicates a possible lack of mass transfer to the electrode surface. This indicates that the bulk concentration could have been too low to properly supply the silver ions to the surface at the rotation rates used. However, the average of the transfer coefficients for 50 and 100 mmol (0.35) matched previous literature exactly [2]. Because of this, to

estimate the exchange current density at 2 M (as is required for the Equation 10), the average rate constants from the 50 and 100 mmol L^{-1} experiments were used. Hence, the average transfer coefficient (0.35) and average rate constant ($13.6 * 10^{-6}$ m s^{-1}) were inserted back into the previous equation shown with the bulk $Ag^{+}_{(aq)}$ concentration to estimate the exchange current density at 2 M to be 18.35 A m^{-2}.

An attempt was made to conduct a Levich analysis on the RDE results in order to estimate the diffusion coefficient of $Ag^{+}_{(aq)}$, but the results showed high variability causing unfeasible results upon linear extrapolation to the concentrations used in the study. Upon review, it has previously been shown that while linear extrapolation through Kohlrausch's Law is applicable for pure $AgNO_3$ for up to concentrations of 2 mol L^{-1}, it is only applicable for pure NH_4NO_3 up to about 0.5 mol L^{-1} [4]. Thus, it is highly unlikely that an electrolyte containing the combination of these two compounds can be linearly extrapolated to the concentrations used in this study. As a result, the diffusion coefficients used in this study were estimated by OLI systems.

Section 2: Method for Estimation of Viscosity

To estimate the viscosity of the electrolyte, an Ubbelohde viscometer (Cannon Instrument Company) was used to compare the elution time of the 2 M $AgNO_3$/5 M NH_4NO_3 electrolyte to that of water. Three measurements were taken to ensure the accuracy of the data acquired.

Table S.2: Trial data for viscometer experiments

Trial	**Water**	**2 M $AgNO_3$/5M NH_4NO_3**
1	155.22	156.17
2	152.35	156.28
3	152.07	156.57
Average	**153.21**	**156.34**

The dynamic viscosity of water is 0.0009 Pa s, and the viscosity of the electrolyte was then calculated by the ratio of the average elution times [5].

$$\mu_{elec} = \mu_{wat} \frac{t_{elec}}{t_{wat}} \tag{S4}$$

$$\mu_{elec} = 0.0009 * \frac{156.34}{153.21} = 0.000918\ Pa\ s$$

Section 3: Full Table of Parameters for Mesh Creation

The mesh that was used for this study was created to provide fine resolution near the boundaries in the positive electrolyte channel and coarse resolution in the negative electrolyte channel (Table S.3). This resulted in multiple layers at the fiber walls in the positive electrolyte channel that grew relatively slowly to the bulk. The transition from the bulk to the boundary layer mesh was smoothed over 8 iterations.

Table S.3: Detailed list of parameters for the creation of the mesh and where they apply to in the model

Parameter	**Value**	**Applies to**
Maximum element size	68.1 μm	Channel 2
Minimum element size	0.305 μm	Channel 2
Maximum element growth rate	1.3	Channel 2
Curvature factor	0.3	Channel 2
Resolution of narrow regions	1	Channel 2
Maximum element size	13.4 μm	Channel 1, bulk
Minimum element size	0.6 μm	Channel 1, bulk
Maximum element growth rate	1.2	Channel 1, bulk
Curvature factor	0.4	Channel 1, bulk
Resolution of narrow regions	1	Channel 1, bulk
Maximum element size	5.6 μm	Channel 1, boundaries
Minimum element size	0.08 μm	Channel 1, boundaries
Maximum element growth rate	1.1	Channel 1, boundaries
Curvature factor	0.25	Channel 1, boundaries
Resolution of narrow regions	1	Channel 1, boundaries
Minimum angle between boundaries	240 deg	Channel 1, boundaries
Element size scaling factor	0.25	Channel 1, boundaries
Number of boundary layers	4	Channel 1, boundaries
Boundary layer stretching factor	1.2	Channel 1, boundaries
Thickness of first layer	0.1 μm	Channel 1, boundaries
Thickness adjustment factor	2.5	Channel 1, boundaries

Section 4: Method for estimation of plugging time

In order to estimate a plugging time for each of the cases studied, the growth velocity at the location that would be the quickest to plug was used along with the spacing between those points or boundaries. For the in-line arrangement, the growth velocity was extracted from the front and back of the cylinders in the top row of the electrode (Figure S.2a). For the staggered arrangement, the growth velocity was extracted from the diagonally-adjacent cylinder surfaces (Figure S.2b).

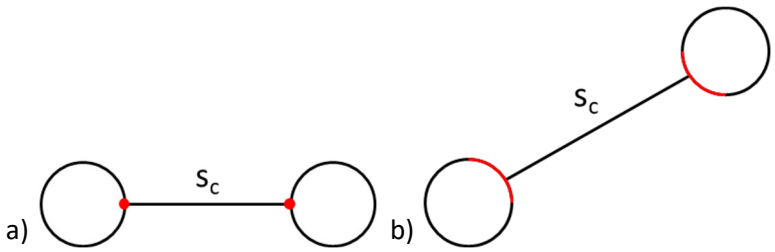

Figure S.2: Cartoon representation of the definition of the spacing used for extrapolating a plugging time of the electrode for a) the in-line arrangement and b) the staggered arrangement. The red indicates the point or boundary that the growth velocity was averaged over for the entire row(s).

The average growth velocity, v_e, for each case was then extrapolated into a plugging time, t_{plug}, by

$$t_{plug} = \frac{s_c/2}{v_{elec}}, \tag{S5}$$

where the column spacing, s_c, was divided in half because the thickness change of the electrode must be half of the spacing for the electrodes to be touching and the pore to be plugged. The average growth velocity was found to vary less than 1% over the simulation time, providing sufficient basis for the value to be extrapolated to much longer times.

References

[1] C. Lim, M.Z. Bazant, III. Reaction Kinetics Lecture 13: Butler-Volmer equation, MIT Opencourseware. (2014). https://ocw.mit.edu/courses/chemical-engineering/10-626-electrochemical-energy-systems-spring-2014/lecture-notes/MIT10_626S14_S11lec13.pdf (accessed June 1, 2020).

[2] S.N. Lvov, Introduction to Electrochemical Science and Engineering, 1st ed., CRC Press, Boca Raton, 2015.

[3] A.J. Bard, L.R. Faulkner, Electrochemical Methods: Fundamentals and Applications, 2nd ed., John Wiley & Sons, Inc., New York, 2001.

[4] G.J. Janz, G.R. Lakshminarayanan, M.P. Klotzkin, G.E. Mayer, Diffusion of silver nitrate in concentrated aqueous solutions, J. Phys. Chem. 70 (1966) 536–539. https://doi.org/10.1021/j100874a036.

[5] D.R. Lide, CRC Handbook of Chemistry and Physics, CRC Press, 1995.